Assessing heart disease using a novel magnetocardiography device

PAPER • **OPEN ACCESS**

Assessing heart disease using a novel magnetocardiography device

Biomedical Physics & Engineering Express

PAPER

Assessing heart disease using a novel magnetocardiography device

R Beadle[1], D McDonnell[1], S Ghasemi-Roudsari[2], L Unitt[2], S J Parker[2] and B T H Varcoe[2,3]

[1] Department of Cardiology, South Warwickshire NHS Foundation Trust, Warwick, United Kingdom
[2] Creavo Medical Technologies, Coventry, United Kingdom
[3] School of Physics and Astronomy, University of Leeds, United Kingdom

E-mail: b.varcoe@leeds.ac.uk

Keywords: magnetocardiography, myocardial infarction, LVEF, ejection fraction

OPEN ACCESS

RECEIVED
28 August 2020

REVISED
27 January 2021

ACCEPTED FOR PUBLICATION
12 February 2021

PUBLISHED
23 February 2021

Abstract

The aim of this paper is to present the use of a portable, unshielded magnetocardiograph (MCG) and identify key characteristics of MCG scans that could be used in future studies to identify parameters that are sensitive to cardiac pathology. We recruited 50 patients with confirmed myocardial infarction (MI) within the past 12 weeks and 46 volunteers with no history of cardiac disease. A set of 38 parameters were extracted from MCG features including both signals from the sensor array and from magnetic images obtained from the device and principal component analysis was used to concentrate the information contained in these parameters into uncorrelated predictors. Linear fits of these parameters were then used to examine the ability of MCG to distinguish between sub-groups of patients. In the first instance, the primary aim of this study was to ensure that MCG has a basic ability to separate a highly polarised patient group (young controls from post infarction patients) and to identify parameters that could be used in future studies to build a formal diagnostic tool kit. Parameters that parameterised left ventricular ejection fraction (LVEF) were identified and an example is presented to show differential low and high ejection fractions.

1. Introduction

Magnetocardiography (MCG) uses an array of non-invasive magnetometers to measure and map the magnetic fields generated by the electrical activity in the heart [1–5]. MCG is non-contact, field free and emission-free, and works through clothing. MCG offers the clinician an alternative view of the heart to conventional ECG [6], which has already led to MCG being useful in the detection of acute coronary ischaemia [7], especially in cases of non-ST segment elevation myocardial infarction (NSTEMI), where MCG has been demonstrated to have a diagnostic advantage.

There are a number of pathways that can lead to heart failure [8] and one of our aims is to develop a diagnostic that would be sensitive to these pathways. Recently we demonstrated that a novel magnetometer array was capable of detecting the cardiac magnetic field in an unshielded clinical setting [9, 10]. An array of 15 room temperature induction magnetometers was used to detect the cardiac magnetic field with a sensitivity of 0.813 $pT\mu V^{-1}$ at 10 Hz and $104fT/\sqrt{Hz}$ noise floor at 10 Hz. In this study we used a prototype device with 37 channels comprised of 19 active sensors and 18 channels used for noise reduction.

As the sensors are inductive, the frequency of the signal is important and for this reason the QRS region has become the main focus of diagnostic development for this device [10]. This is a departure from previous MCG studies which have focused on the S-T and T region (see for example) [10–14]. However, that is not to say that the QRS region has no diagnostic value as a number of papers have also demonstrated a good diagnostic performance extracting parameters from the QRS region [15–23].

The primary aim of the current study however, has a somewhat more modest goal; namely to ensure that we were able to distinguish signals from a small polarised sample of patients. In this case the aim is to separate young controls and post infarction patients as the first step in the development of a tool kit of diagnostic parameters. A secondary aim was to find signals that would indicate declining cardiac function, expected in a population following myocardial infarction (MI).

With such a small sample of patients we are faced with the difficulty of having insufficient numbers of

patients to allow the development and testing of a model, hence we restricted our search to identifying indicators that were correlated to the conditions of interest. The analysis of the data presented in this paper uses tools and principal components developed during a recent 700 patient multicentre clinical trial [24].

2. Method

This study explored the MCG findings in participants who had had a confirmed myocardial infarction (MI) in the prior 12 weeks and compared these findings to scans acquired separately from a population of young volunteers with no history of heart disease. Patients (n = 50) were consecutively recruited from the South Warwickshire NHS Foundation Trust wards and cardiac rehabilitation programme. All patients had been diagnosed as having had an MI based on clinical assessment and biochemical markers in accordance with European Society of Cardiology Guidance [25]. To be included in the study the patient must have been within 12 weeks of the initial event and willing to give consent. Patients with atrial fibrillation, thoracic metal implants, pacemakers or implantable cardioverter defibrillators were excluded. Patients also needed to be able to lay flat for the examination. Pregnant or peripartum patients were also excluded. Patient's medical records were reviewed to help better define the population characteristics. The young healthy control (YHC) population was used because of the low prevalence of heart disease in a population below the age of 35. No cardiac tests were performed on the YHC population. All participants provided written informed consent, and research was performed in accordance with the Declaration of Helsinki and BS EN ISO 14155:2011, Clinical Investigation of Medical Devices for Human Subjects—Good Clinical Practice. The study was approved by the South West Research Ethics Committee (17/SW/0293).

The MCG was performed by a trained and experienced operator in accordance with the manufacturer's instructions for use (Vitalscan device, Creavo Medical Technologies). Each scan took approximately 5 minutes to acquire. Other than for removing bulky clothing or clothing containing metal, patients remained fully clothed with ECG electrodes placed on the patient's wrists and left ankle during the scan.

The sensor head uses 37 sensors in a hexagonal array (figure 1). Nineteen (19) inner coils are used to sample the magnetic field of the patient and the outer ring of 18 coils are used for noise reduction. Figure 2 shows the traces obtained from each location. At a single point in time (a position along the *x*-axis of figure 2) the field intensity can be represented as a two dimensional magnetic field map (the red and blue regions in figure 1). The field map allows us to add another dimension to the data by looking at the spatial correlations between the signals.

The detectors measure the rate of change of the magnetic field, therefore, lower frequency signals tend to be suppressed and the signal is a 'performance measure' of the depolarisation taking into account both the duration and amplitude of the depolarisation signal.

3. Results and discussion

Fifty (50) patients (39 male, 11 female) with a mean age of 63.51 years were consented and enrolled into the study from the cardiology wards and rehabilitation classes, following admission to the cardiology wards at the South Warwickshire NHS Foundation Trust (Warwick hospital). All patients had a confirmed MI (13 STEMI, 37 NSTEMI) within the 12 weeks prior to consent (range 1 day to 10.57 weeks). The majority of patients were white caucasian with an anterior MI being the most prevalent region of MI. Eighteen (18) patients (36%) received medical management only whilst all other patients underwent percutaneous coronary intervention (PCI) with 1 patient undergoing 2 procedures. MCG scans were taken on 45 patients (2.29 to 12.14 weeks post MI) as 5 patients were unable to be scanned (3 died between time of consent and date of the scan (1 before discharge) and 2 patients withdrew from the study before the scan was taken due to increasing illness. These data were compared to that of a young healthy group of volunteers (30 male, 16 female) with a mean age of 22.48 and no history of heart disease. Further details on participant demographics and diagnosis and treatment of the post MI group can be seen in tables 1 and 2 respectively.

Several variables that are potentially of interest were identified and extracted from the MCG scan data and image data. The parameters that were extracted are presented in table 3 and details the 38 parameters extracted from the MCG data. Tables 4 and 5 present the outcomes of measurements of the MCG parameters for all 38 parameters and the p-value comparing post MI and YHC volunteer data. From here, we find that ten parameters show a significant difference ($p < 0.05$) between the post MI and YHC populations (parameters highlighted in bold).

Model building on ten parameters would require around 150 participants, however given the descriptions of these parameters (table 3) it is highly likely that these parameters are correlated with each other. For this reason, Principal Component Analysis (PCA) was selected as a stratagem that could produce a set of uncorrelated predictors. PCA is a method of reducing the dimensionality of a dataset while minimising information loss. It does so by creating a new set of uncorrelated variables called principal components (PCs).

Before generating the principal components, MCG predictors are passed through a regularisation proceedure to produce a set of values with consistent gaussian distributions. The parameters were derived

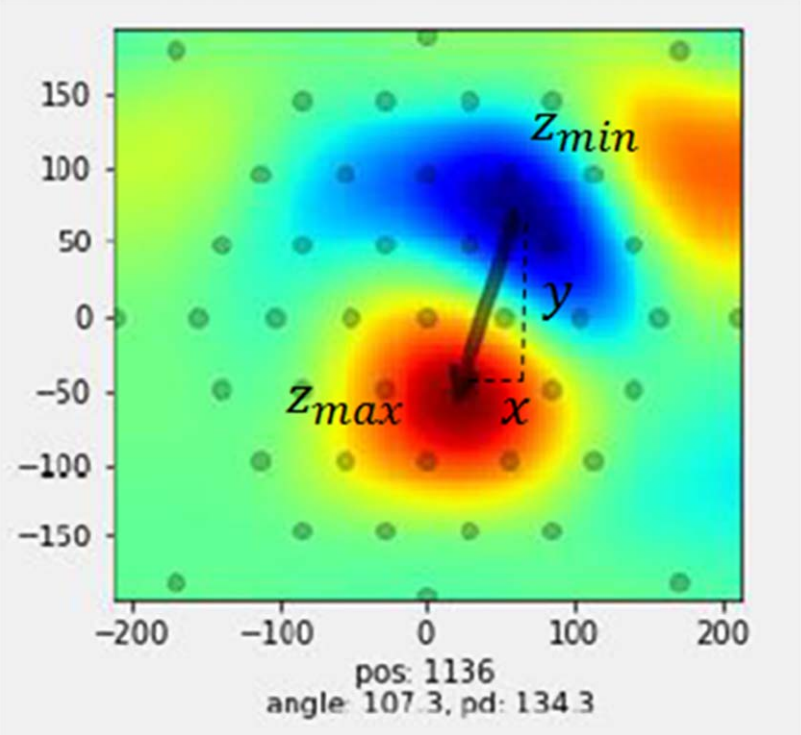

Figure 1. The colour map is a representation of the magnetic field detected by the sensors in the array. The outer ring of sensors is disabled for this view. A vector is drawn between the maximum and minimum magnetic field Zmax and Zmin respectively. Grey dots in in the center of the image show the position of sensor. Grey dots in the outer boundary represent part of the image reconstruction map.

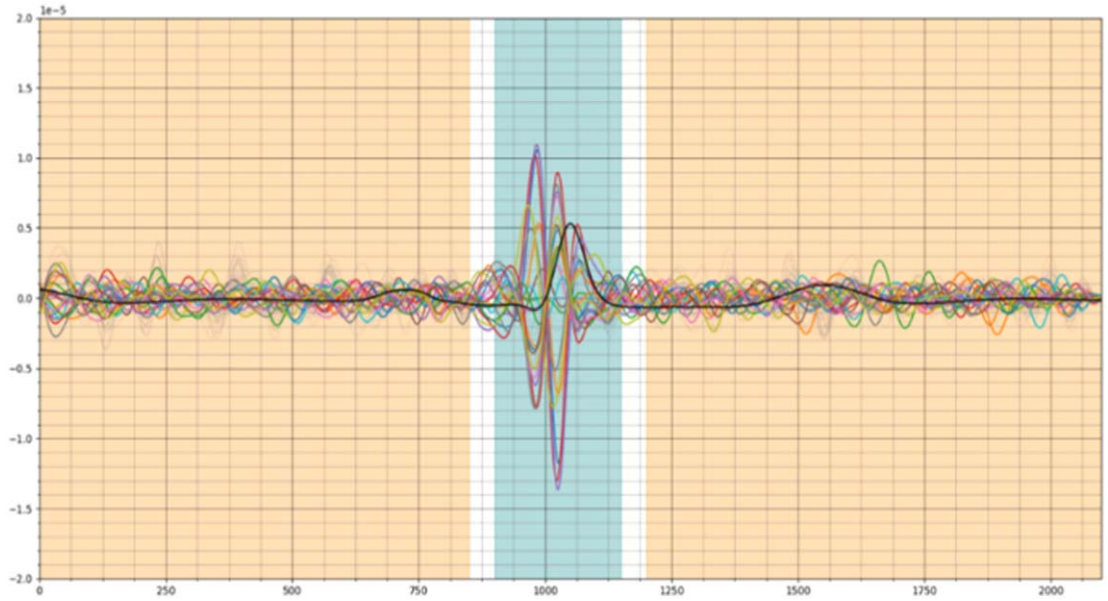

Figure 2. The individual traces from the 19 sensor coils in the array overlaid with a concurrent ECG (black). The central region highlights the focal region for parameter extraction.

using the methods outlined in [24]. Principal component analysis is often used in machine learning, however, in the current work this was a device to determine which of the MCG parameters were uncorrelated indicators.

For example in tables 4 and 5 there are 10 variables that all show a statistically significant difference between the post MI patients and YHC populations. In examining PCA analysis we find that a single variable, PC1 (the first principal component), contains all 10 of

Table 1. Subject Demographics.

Description	Category	Post MI Study Group (n = 50)	Post MI Analysis Group (n = 45)	YHC Analysis Group (n = 46)
Gender	Male	39 (78%)	38 (84.44%)	30 (32.62%)
	Female	11 (22%)	7 (15.56%)	16 (34.78%)
Age	Age range (yrs)	37.41–89.03	37.41–85.90	18–29
	Mean age (yrs)	63.51	61.30	22.48
Ethnicity	White Caucasian	47 (94%)	42 (93.33%)	—
	Asian/Asian British	3 (6%)	3 (6.67%)	—

Table 2. Post MI Group Diagnosis and Treatment.

Location of MI	Number	Vessel (those patients undergoing PCI)	Number
Anterior	17	Circumflex	3
Inferior	14	Left Anterior Descending	17*
Lateral	2	Right Coronary Artery	12*
Posterior	1	Other	1
Undiagnosed	16	*1 patient underwent 2 PCI procedures	

these variables. The components RS_max, QR_max, QR_min, RS_min, QR_PKMn, RS_PKMn, QR_PK, QR_PKMx, RS_PK, and RS_PKMx along with two additional components, RS_PKD and QR_PKD, represent the 12 most significant elements of PC1 [26]. Therefore we used PC1 as an Ersatz variable for this collection of variables.

Two risks that can adversely influence this choice are (1) that the coefficients are proportional to the mean of the variable set and (2) that the correlation present in the data are purely coincidental. To circumvent these risks the Ps were created using the data set presented in [24], and therefore the association between the prominance of these elements with high levels of correlation in the current experiment indicate that this is real.

A predictive model was therefore created based solely on PC1. No 'machine learning' or curve fitting is required for this as it is a single parameter. However, we converted the parameter to a probability score using the formula $1/(1 + \mathrm{Exp}(M))$, and therefore we scaled the principal component to give a range of probabilities from zero to one using the following scaling,

$$M = -0.85 + 0.4PC1 \quad (1)$$

The results for the scaling in equation (1) are presented in figure 3, which illustrates the model outcomes and an ROC curve for predictions based on the single parameter model. The AUC is 95% and for a cut point of 0.57 gives a sensitivity and specificity of 100% (95% CI: 92.89% to 100.00%) and 76% (95% CI: 58.87% to 85.73%) respectively. This is a remarkable result as it could be read as a predictive indication. However, given that the two populations were already highly polarised it is not immediately clear what the reason for this difference is.

There are many reasons why cardiac function would decline with age, however, the most obvious difference that we see in the data would be a reduction in left ventricular ejection fraction (LVEF) in the post MI group relative to the young control group. As a summary measure of cardiac function, LVEF also has the benefit of being a useful indicator for comparison.

Moreover, there must be a reason in the electrophysiology of the heart. That is, there must be signals that are detectable with an MCG that can explain the difference observed in figure 3. Indeed the feature that we would expect to be different between the YHC and Post MI group is the LVEF and while we do not have LVEF data from the young control group, we do have data from the post MI group.

The link between LVEF and the most important components of PC1 would most likely come through heart muscle volume. The MCG QRS signal would most likley be larger when there is more muscle involved in generating the signal. This would also fit with observations made in refs. [15, 21, 23, 27–30] in which it was observed that changing the blood flow to the heart results in changes to the QR and RS slopes. These slopes correspond to the QR and RS MCG parameters present in PC1.

A limitation of LVEF is that it contains a significant element of operator judgment with a 95% confidence interval of at least ±10% [31] depending on the method used. Nevertheless, this parameter is frequently used to determine downstream risk to the patient [31, 32]. A second limitation is the way the data for LVEF was recorded within the database obtained from source data. The tendency is to simply note that the LVEF was greater than 55% as this indicates low cardiac risk.

Returning to data analysis, based on refs [21–23, 30, 33–36] we anticipate that PC1 contains some elements that are related to LVEF [21–23, 30, 33–36]. In that case we would assume that a model can be constructed that would be able to discriminate LVEF in the post MI group. As a check, we anticipate that the YHC group would have higher, average LVEF than the post MI group and the MCG should agree with that prediction.

PC2 and PC33 were selected to work adjunctively with PC1 for the LVEF model. The variance of PC2 is

Table 3. Magnetocardiography parameters and definitions.

Full name (unit)	Definition	Related parameters
Field map angle (degree)	Angle between negative and positive pole.	QR_MA, RS_MA
Pole Distance (mm)	Distance between negative and positive pole.	QR_PD, RS_PD,
Maximum to minimum ratio (no unit)	Amplitude ratio between the negative and the positive pole.	QR_MMR, RS_MMR,
Peak to peak amplitude difference	Amplitude difference between the positive and negative pole.	QR_PK, RS_PK,
Map angle vector statistics (degrees)	Maximum of field map angles within an interval.	QR_MAMx, RS_MAMx,
	Minimum of field map angles within an interval.	QR_MAMn, RS_MAMn
Pole distance vector statistics (mm)	Maximum of pole distances within an interval.	QR_PDMx, RS_PDMx,
	Minimum of pole distances within an interval.	QR_PDMn, RS_PDMn
Ratio vector statistics (no unit)	Maximum of MMR within an interval.	QR_RMx, RS_RMx,
	Minimum of MMR within an interval.	QR_RMn, RS_RMn
Peak vector statistics (mV)	Maximum of peak to peak differences within an interval.	QR_PKMx, RS_PKMx,
	Minimum of peak to peak differences within an interval.	QR_PKMn, RS_PKMn,
Map angle dynamics (degree)	Maximum change of the map angle within 10 taps/samples.	QR_MAD, RS_MAD,
Distance dynamics (mm)	Maximum pole distance change within 10 taps/samples.	QR_PDD, RS_PDD,
Ratio dynamics (no unit)	Maximum ratio change within 10 taps/samples.	QR_RD, RS_RD
Peak dynamics (mV)	Maximum pole distance change within 10 taps/samples.	QR_PKD, RS_PKD
Field map angle (degree)	Angle between negative and positive pole.	QR_MA, RS_MA
Pole Distance (mm)	Distance between negative and positive pole.	QR_PD, RS_PD,
Maximum to minimum ratio (no unit)	Amplitude ratio between the negative and the positive pole.	QR_MMR, RS_MMR,

Table 4. Summary statistics of the data collected for parameters relating to the R-S transition in the magnetic field analysis. Five parameters show a potentially significant change between the two populations.

	IHD		YHC		
Parameter	Mean	Std	Mean	Std	p-value
RS_MA	-70.03842558	29.18257296	-53.47490455	55.04531386	0.092068516
RS_MAD	-0.551188372	23.18628822	0.279679545	31.48700167	0.153553836
RS_MAMn	-80.00053953	32.03990404	-76.54018182	35.26454701	0.142889328
RS_MAMx	-59.09279302	32.72426825	-55.61751818	38.4832127	0.14314583
RS_MMR	0.987402326	0.152019452	1.039075	0.137758501	0.113871036
RS_PD	153.1917599	17.69347207	142.2381761	16.00104964	0.277974662
RS_PDD	4.300697674	14.73558879	0.135559091	17.53168007	0.21016395
RS_PDMn	144.641	17.31972984	134.7643227	13.54166315	0.268688487
RS_PDMx	161.2755512	16.04050401	150.525075	18.235955	0.287085679
RS_PK	2.34E-05	8.64E-06	8.74E-05	3.71E-05	0.004440428
RS_PKD	1.18E-06	5.35E-06	3.55E-06	2.17E-05	0.103272861
RS_PKMn	0.0000188	6.71E-06	6.79E-05	2.92E-05	0.004535637
RS_PKMx	2.36E-05	8.64E-06	8.82E-05	3.76E-05	0.004357224
RS_RD	0.017776744	0.129180846	0.033490909	0.140749598	0.140964414
RS_RMn	0.903497674	0.129610117	0.968206818	0.11974977	0.098008436
RS_RMx	1.057913953	0.176985076	1.134847727	0.169944952	0.104079384
RS_cursor	1033.255814	8.707369301	1032.545455	5.331955745	0.172666744
RS_max	1.16E-05	4.49E-06	4.39E-05	1.78E-05	0.004671563
RS_min	-1.18E-05	4.34E-06	-4.35E-05	1.97E-05	0.007812767

Table 5. Summary statistics of the data collected for parameters relating to the Q-R transition in the magnetic field analysis. Five parameters show a potentially significant change between the two populations.

	IHD		YHC		
Parameter	Mean	Std	Mean	Std	p-value
QR_MA	103.3185	31.25311323	94.61558636	56.87583204	0.20933011
QR_MAD	3.807439535	24.48343472	2.291468182	22.41310511	0.169314006
QR_MAMn	91.90053023	32.40187627	85.67134773	59.60664604	0.19262743
QR_MAMx	113.0924349	32.07064859	105.1845955	56.72411862	0.203049294
QR_MMR	1.031932558	0.166700196	1.035984091	0.158434868	0.155333785
QR_PD	156.6356167	17.22944932	142.5139718	20.04622768	0.308279689
QR_PDD	-1.305627907	20.7633803	-0.888456818	21.8206282	0.155989371
QR_PDMn	146.2664535	16.31084345	130.3366068	13.29975252	0.318136305
QR_PDMx	166.2436953	17.30524557	148.7027841	20.72064763	0.318250865
QR_PK	2.14E-05	8.72E-06	7.18E-05	3.10E-05	0.006777466
QR_PKD	-2.35E-07	5.10E-06	-1.50E-07	1.84E-05	0.156527531
QR_PKMn	1.73E-05	6.60E-06	5.60E-05	2.42E-05	0.006616362
QR_PKMx	2.16E-05	8.75E-06	0.000072975	3.19E-05	0.006617833
QR_RD	-0.024167442	0.172217426	0.027086364	0.194999365	0.118604424
QR_RMn	0.94782093	0.144403766	0.938372727	0.124365585	0.169908191
QR_RMx	1.141974419	0.203990409	1.166365909	0.212452928	0.141255041
QR_cursor	984.0232558	9.463487661	986.7045455	6.27976384	0.12025599
QR_max	1.07E-05	4.16E-06	3.66E-05	1.73E-05	0.005981636
QR_min	-1.07E-05	4.75E-06	-3.51E-05	1.43E-05	0.017405312

mostly accounted for by six parameters QR_MMR, QR_RMn, QR_RMx, RS_MMR, RS_RMn, and RS_RMx. These are ratio parameters that indicate distortion of one side of the cardiac signal. They are present with approximately equal weight, but opposite sign for the QR and RS transitions. This indicates that all three QR and RS indicators are actually only measuring a single value. Similar parameters have been used in the past for the detection of ACS [4, 37, 38]. The variance of PC33 is mostly accounted for by four parameters QR_PKMn, QR_PKMx, RS_PKMn and RS_PKMx (the most significant predictors in tables 4 and 5, with the split 3:1 between the RS and QR components [RS components dominating]). This parameter is therefore

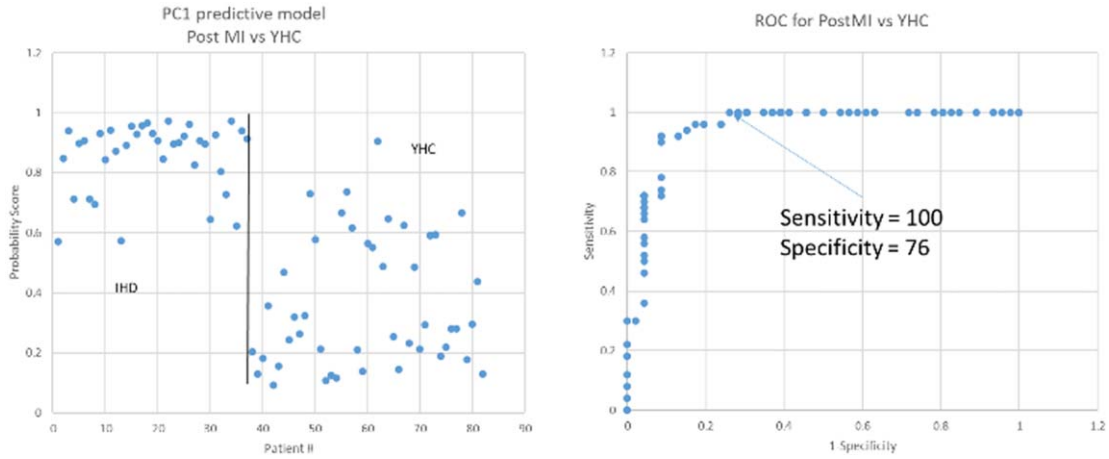

Figure 3. The figure on the left shows the distribution of the PC1 based probability score versus patient number for post MI and YHC patients. The figure on the right shows the ROC curve obtained for this distribution. The AUC is 95% and for a cut point of 0.57 the Sensitivity and Specificity of 100% (95%CI: 92.89% to 100.00%) and 76% (95% CI: 58.87% to 85.73%) respectively.

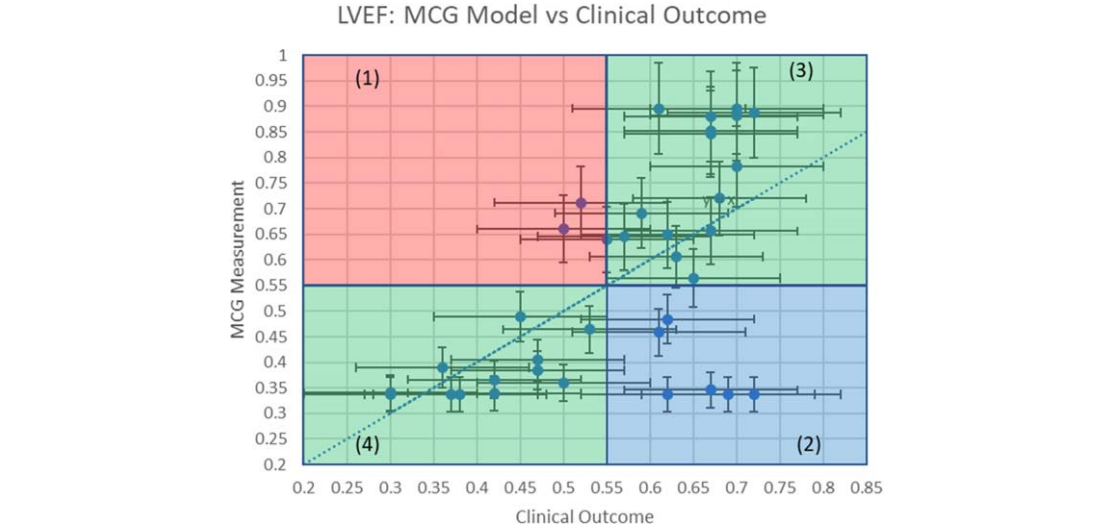

Figure 4. MCG model of LVEF versus clinical determination. The four regions are: (1) in Red, Mischaracterisation error, reducing patient risk; (2), and (3), in Green, patient accurately characterised; (4) in Blue, Patient mischaracterised as higher risk. The dotted line indicates the curve y=x. Error bars for clinical evaluation are ±10% and the statistical standard deviation of the MCG measurement.

closely related to the parameters used in [33] which has previously demonstrated a link between depolarization and LVEF. The use of such a high valued PC would not be normal if we were performing machine learning for example. However, in the present experiment, we are seeking to optimise for parameters that are known to be sensitive to LVEF, hence the choice of an otherwise unusually high valued PC.

A linear regression curve fit to LVEF data taken from the post MI patient group produces the equation:

$$M = -1.7 - 0.85PC1 - 0.58PC2 + 27PC33. \quad (2)$$

Based on this curve fit, we can assess the performance of the model against the LVEF data that we hold for the patients. The outcome of this comparison is presented in figure 4. Horizontal error bars assume a 10% error in measurements of LVEF (see ref [30]) and vertical error bars represent the average standard deviation of MCG results as a percentage error from the fit. For the purpose of this comparison the model output data is remapped onto the line y = x using the transformation $Y = -0.6 + 1.8X$ in order to assess the clinical prediction capability of the model.

Limitations of the curve fit: The model is based on three parameters which for 36 patients gives 12 patients per predictor. This means that we cannot perform a conventional train-test split and the only testing group is the YHC cohort. Also, as noted above, there are substantial errors associated with the collection of LVEF data, due to operator variability, the timing of data collection and the variable methods of determining the LVEF. The clinical data becomes less accurate above 55% because of changes in reporting. Both of these limiations mean that 'ground truth' is not well defined.

Table 6. Clinical prediction against an LVEF of 55% for the MCG model.

Sensitivity	85.71%	57.19% to 98.22%
Specificity	72.73%	49.78% to 89.27%
Positive Likelihood Ratio	3.14	1.54 to 6.43
Negative Likelihood Ratio	0.2	0.05 to 0.73
Positive Predictive Value	66.67%	49.45% to 80.35%
Negative Predictive Value	88.89%	68.37% to 96.73%
Accuracy	77.78%	60.85% to 89.88%

Nevertheless, the results are in line with previous investigations that used parameters based on dynamical changes during depolarisation as a measure of left ventricular function. Moreover, we can assign three basic clinical outcomes that would result from an MCG determination of the LVEF. These are indicated as the four quadrants (labelled, 1,2,3,4) in figure 4. In quadrants labelled 1,2 the clinical outcome would have been altered; patients in quadrant 1 are given a higher value of LVEF with MCG than the clinical assessment; patients in quadrant 2 are given a lower value of LVEF than clinically assesed. Patients in quadrants 3,4 are unchanged.

The MCG prediction departs significantly from the clinical outcome for measurements above 55%. This is a result of the reporting limitations that scores of simply '>55%' are indicated in patient medical notes. Where this occurs the patient score has been entered as 70% for the purpose of this graph. A second limitation of reporting is the tendancy to report a range of possible values (e.g. 55%–60%) and where this occurs the patient has been assigned the mid point of the range for the graph.

Assessing the patients in a binary outcome against the score of 55% gives the outcomes presented in table 6. A note of caution here is that the outcome is not binary and ground truth is not well defined, hence this is only a measure of the ability of MCG to reproduce the reported outcomes. The error of the prediction is therefore limited by the LVEF reporting. There are many reasons that there would be a difference between the two groups The most likely difference however, is ejection fraction and it is worth noting that the YHC group have a higher average 'prediction' than the post MI group.

Despite the limitations, these results are nevertheless sufficently interesting that they warrant further investigation and would suggest that a formal clincial investigation is warranted.

4. Summary

In summary, we have developed a set of predictors that have captured a large range of diversity of cardiac signals. We have applied these parameters to assess the ability of MCG to recover an important factor in monitoring cardiac health. This is interesting because LVEF is a measure of the performance of the heart in pumping blood and prior to this observation one may have said that the two are unrelated. However, the volume and activity of heart muscle will contribute more to the MCG signal than other more subtle changes would. Hence the connection is probably more fundamental than it would otherwise appear, with younger healthier hearts with more active muscle contributing to the magnetic signal more than post-infarction hearts.

That being said, we must also note that the LVEF input data is noisy and the current outcome therefore has only a limited application at this stage. However, as mentioned above, the measurement of LVEF is an important, and relatively expensive [39], parameter to acquire. It is a key element in assessing cardiac function, revealing information that is almost inaccessible to any other measurement. For this reason looking for a method that could rapidly assess a patient would be worth while. A future study with a larger patient group and more accurate data (for example using SPECT) would be recommended.

Data availability statement

The data generated and/or analysed during the current study are not publicly available for legal/ethical reasons but are available from the corresponding author on reasonable request.

ORCID iDs

B T H Varcoe https://orcid.org/0000-0001-7056-7238

References

[1] Weber Dos Santos R *et al* 2004 MCG to ECG source differences: measurements and a two-dimensional computer model study *Journal of Electrocardiology* **37** 123–7
[2] Tolstrup K *et al* 2006 Non-invasive resting magnetocardiographic imaging for the rapid detection of ischemia in subjects presenting with chest pain *Cardiology* **106** 270–6
[3] SMars P A *et al* 2005 Magnetocardiography as a diagnostic tool to determine ischemic heart disease in patients presenting with chest pain *Annals of Emergency Medicine* **46** 43
[4] Park J-W *et al* 2005 Magnetocardiography predicts coronary artery disease in patients with acute chest pain *Annals of Noninvasive Electrocardiology* **10** 312–23
[5] Fenici R, Brisinda D and Meloni A M 2005 Clinical application of magnetocardiography *Expert Reviews in Molecular Diagnostics* **5** 291-313
[6] Alday E A P *et al* 2016 Comparison of electric- and magnetic-cardiograms produced by myocardial ischemia in models of the human ventricle and torso *PLoS One* **11** e0160999
[7] Camm A. John, Henderson Robert, Brisinda Donatella, Richard Body, Richard G. Charles, Varcoe Ben and Fenici Riccardo 2019 Clinical utility of magnetocardiography in cardiology for the detection of myocardial ischemia *Journal of Electrocardiology* **57** 10–17
[8] Li H *et al* 2020 Targeting age-related pathways in heart failure *Circ. Res.* **126** 533–51

[9] Mooney J W et al 2017 A portable diagnostic device for cardiac magnetic field mapping Biomed. Phys. Eng. Express 3 015008
[10] Ghasemi-Roudsari S et al 2018 A portable prototype magnetometer to differentiate ischemic and non-ischemic heart disease in patients with chest pain PLoS One 13 e0191241
[11] Schless B G et al 2004 Analysis of the ST-segment in terms of principal components: application on multichannel magnetocardiographic recordings J. Med. Eng. Technol. 28 56–60
[12] Park J-W et al 2008 Resting magnetocardiography predicts 3-Year mortality in patients presenting with acute chest pain without ST segment elevation Annals of Noninvasive Electrocardiology 13 171–9
[13] Kim B-S, Uchikawa Y and Kobayashi K 2007 Analysis of ST segment of exercise-induced MCG based on 3D vector measurement International Congress Series 1300 500–3
[14] Hailer B et al 2003 Magnetocardiography in coronary artery disease with a new system in an unshielded setting Clinical Cardiology 26 465–71
[15] Yıldırım E et al 2013 Relationship between left ventricular ejection fraction and number of fragmented QRS complex derivations on standard 12-lead electrocardiogram in acute ST-elevated myocardial infarction patients Journal of the American College of Cardiology 62 C8–9
[16] Bailón R et al 2003 Coronary artery disease diagnosis based on exercise electrocardiogram indexes from repolarisation, depolarisation and heart rate variability 41 561–71
[17] Alvi R et al 2016 Athens QRS score as a predictor of coronary artery disease in patients with chest pain and normal exercise stress test J. Am. Heart Assoc. 5 e002832
[18] Korhonen P et al 2001 Magnetocardiographic Intra-QRS fragmentation analysis in the identification of patients with sustained ventricular tachycardia after myocardial infarction Pace-Pacing and Clinical Electrophysiology 24 1179–86
[19] Ringborn M et al 2010 Comparison of high-frequency QRS components and ST-segment elevation to detect and quantify acute myocardial ischemia Journal of Electrocardiology 43 113–20
[20] Surawicz B et al 1997 QRS changes during percutaneous transluminal coronary angioplasty and their possible mechanisms Journal of the American College of Cardiology 30 452–8
[21] Romero D et al 2016 Ischemia detection from morphological QRS angle changes Physiol. Meas. 37 1004–23
[22] Romero D et al 2012 Characterization of ventricular depolarization and repolarization changes in a porcine model of myocardial infarction Physiol. Meas. 33 1975–91
[23] Romero D et al 2013 Detection and quantification of acute myocardial ischemia by morphologic evaluation of QRS changes by an angle-based method Journal of Electrocardiology 46 204–14
[24] Goodacre S et al 2021 Diagnostic accuracy of the magnetocardiograph for patients with suspected acute coronary syndrome Emergency Medicine Journal 38 47–52
[25] Roffi M et al 2016 2015 ESC Guidelines for the management of acute coronary syndromes in patients presenting without persistent ST-segment elevation: task force for the management of acute coronary syndromes in patients presenting without persistent ST-segment elevation of the european society of cardiology (ESC) Eur. Heart J. 37 267–315
[26] Hunsiker E 2018 Loughborough Univeristy, performed independent PCA analysis and provided lists of component value contributions used here
[27] Rosengarten J A et al 2013 Can QRS scoring predict left ventricular scar and clinical outcomes? EP Europace 15 1034–41
[28] Kawakami S et al 2012 Fragmented left ventricular activation on magnetocardiography can predict adverse cardiac events in dilated cardiomyopathy patients with narrow QRS duration Circulation 126 A12431
[29] Mensah-Brown N A et al 2010 Assessment of left ventricular pre-ejection period in the fetus using simultaneous magnetocardiography and echocardiography Fetal Diagnosis and Therapy 28 167–74
[30] Romero D et al 2011 Depolarization changes during acute myocardial ischemia by evaluation of QRS slopes: standard lead and vectorial approach IEEE Trans. Biomed. Eng. 58 110–20
[31] Pellikka P A et al 2018 Variability in ejection fraction measured by echocardiography, gated single-photon emission computed tomography, and cardiac magnetic resonance in patients with coronary artery disease and left ventricular dysfunction JAMA Netw Open 1 e181456
[32] Sutton N R et al 2016 The association of left ventricular ejection fraction with clinical outcomes after myocardial infarction: findings from the Acute Coronary Treatment and Intervention Outcomes Network (ACTION) Registry–Get With the Guidelines (GWTG) Medicare-linked database Am. Heart J. 178 65–73
[33] Palmeri S T et al 1982 A QRS scoring system for assessing left ventricular function after myocardial infarction The New England Journal Of Medicine N Engl J Med 306 4–9
[34] Daniel R et al 2012 Characterization of ventricular depolarization and repolarization changes in a porcine model of myocardial infarction Physiol. Meas. 33 1975
[35] Ringborn M et al 2011 Evaluation of depolarization changes during acute myocardial ischemia by analysis of QRS slopes Journal of Electrocardiology 44 416–24
[36] Lázaro J et al 2013 Electrocardiogram derived respiration from QRS slopes: evaluation with stress testing recordings Computing in Cardiology 2013 655-658 in
[37] Kandori A et al 2001 A method for detecting myocardial abnormality by using a current-ratio map calculated from an exercise-induced magnetocardiogram Med. Biol. Eng. Comput. 39 29–34
[38] Wagner G S et al 1982 Evaluation of a QRS scoring system for estimating myocardial infarct size. I. Specificity and observer agreement Circulation 65 342–7
[39] Anthony F Y et al 2017 Cost-Effectiveness of Cardiotoxicity Monitoring. Aug 14 Available from (https://acc.org/latest-in-cardiology/articles/2017/08/14/07/23/cost-effectiveness-of-cardiotoxicity-monitoring)
[40] Camm A John, Henderson Robert, Brisinda Donatella, Body Richard, Charles Richard G, Varcoe Ben and Fenici Riccardo 2019 Clinical utility of magnetocardiography in cardiology for the detection of myocardial ischemia Journal of Electrocardiology 57 10–17